European Journal of Radiology 110 (2019) 39–44

Contents lists available at ScienceDirect

European Journal of Radiology

journal homepage: www.elsevier.com/locate/ejrad

Research article

Comparison of patient dose from routine multi-phase and dynamic liver perfusion CT studies taking into account the effect of iodinated contrast administration

Kostas Perisinakis[a,b,*], Antonis Tzedakis[b], Styliani Pouli[c], Kostas Spanakis[c], Adam Hatzidakis[c,d], John Damilakis[a,b]

[a] Department of Medical Physics, Medical School, University of Crete, P.O. Box 2208, Heraklion 71003, Crete, Greece
[b] Department of Medical Physics, University Hospital of Heraklion, P.O. Box 1352, Heraklion 71110, Crete, Greece
[c] Department of Radiology, University Hospital of Heraklion, P.O. Box 1352, Heraklion 71110, Crete, Greece
[d] Department of Radiology, Medical School, University of Crete, P.O. Box 2208, Heraklion 71003, Crete, Greece

ARTICLE INFO

Keywords:
Multidetector computed tomography
Liver
Perfusion imaging
Radiation dosage

ABSTRACT

Objectives: To accurately determine and compare patient radiation burden from routine multi-phase CT (MPCT) and dynamic CT liver perfusion (CTLP) studies taking into account the effect of iodine uptake of exposed tissues/organs.

Materials and Methods: 40 consecutive MPCT of upper abdomen and 40 consecutive CTLP studies performed on a modern CT scanner were retrospectively studied. Iodine uptake of radiosensitive tissues at the time of acquisition was calculated through the difference of tissues' CT numbers between NECT and CECT images. Monte Carlo simulation and mathematical anthropomorphic phantoms were employed to derive patient-size-specific organ dose data from each scan involved taking into account the effect of iodinated contrast uptake on absorbed dose. Effective dose estimates were derived for routine multiphase CT and CTLP by summing up the contribution of NECT and CECT scans involved.

Results: The mean underestimation error in organ doses from CECT exposures if iodine uptake is not encountered was found to be 2.2%–38.9%. The effective dose to an average-size patient from routine 3-phase CT, 4-phase CT and CTLP studies was found to be 20.6, 27.7 and 25.8 mSv, respectively. Effective dose from CTLP was found lower than 4-phase CT of upper abdomen irrespective of patient body size. Compared to 3-phase CT, the radiation burden from CTLP was found to be higher for average size-patients but again lower for overweight patients.

Conclusions: Modern CT technology allows CTLP studies at comparable or even lower patient radiation burden compared to routine multi-phase liver CT imaging.

1. Introduction

Multiphase contrast enhanced CT (MPCT), comprised of an un-enhanced scan followed by scans at arterial, portal and occasionally equilibrium phase, has been routinely utilized for the detection or/and follow-up of liver tumors [1]. However, multiphase CT imaging may not exploit maximum arterial enhancement resulting in suboptimal depiction of lesions [1]. Apart from addressing this issue, dynamic CT liver perfusion (CTLP) has been reported to provide unique information regarding microcirculation of focal liver lesions against non-tumorous parenchyma [1–3]. Despite concerns regarding patient radiation burden and technical limitations, CTLP has been progressively featured as a valuable alternative tool for assessing anti-cancer treatment efficacy as well as for diagnosing primary or metastatic tumors [1–3]. Recent technological advances in CT imaging, allowed CTLP to reach technical maturity, since limitations regarding inadequate coverage, temporal resolution and motion-related artifacts have been sufficiently addressed in modern fast multi-detector CT scanners [1,2]. Besides, the use of low tube voltage for acquisition in association with advanced reconstruction algorithms has been proven to allow considerable

Abbreviations: CTLP, CT liver perfusion; MPCT, multi-phase CT; NECT, non-enhanced CT; CECT, contrast enhanced CT; CTDI, CT dose index; DLP, dose length product; % w/w, % weight per weight

* Corresponding author at: University of Crete, Medical School, Medical Physics Department, P.O. Box 2208, 71003 Heraklion, Crete, Greece.
E-mail address: kostas.perisinakis@med.uoc.gr (K. Perisinakis).

https://doi.org/10.1016/j.ejrad.2018.11.015
Received 6 June 2018; Received in revised form 15 November 2018; Accepted 18 November 2018
0720-048X/

reduction of radiation exposure involved in CTLP, thus, reducing the gap between liver CT perfusion and standard multi-phase CT imaging of the upper abdomen regarding patient radiation burden [4]. However, radiation related concerns still exist since patient effective dose from CTLP may occasionally exceed 30 mSv even for modern CT systems [5].

Radiation burden from multi-phase liver CT and CTLP studies has been reported by several investigators in terms of effective dose estimated through the dose-length product (DLP) of the examination [6–9]. However, determination of absorbed dose to each exposed radiosensitive organ and organ dose-based calculation of effective dose is considered more reliable method to quantify radiation risk from CT exposures [10–12]. There are few publications reporting organ doses from liver CT examinations derived by Monte Carlo simulation of CT exposures on mathematical anthropomorphic phantoms [4,5]. Organs/tissues in mathematical phantoms are customarily represented with standard density and elemental composition to mimic corresponding human tissues. However, the iodine tissue-uptake during contrast-enhanced CT imaging has been recently reported to considerably affect the radiation dose absorption on tissues/organs from CT exposures [13]. For the same CT exposure, iodinated tissues were reported to receive up to 100% higher radiation dose with dose increase being proportional to iodine uptake. As a consequence, Monte Carlo-derived dosimetric data regarding contrast enhanced CT imaging may suffer considerable underestimation errors if the iodine-induced change in elemental composition of organs/tissues is not taken into consideration.

The aim of this study was to determine and compare organ-specific dosimetric data from routine multiphase-phase liver CT and dynamic liver perfusion CT studies, taking into account the iodine uptake to organs/tissues during involved exposures.

2. Materials and methods

2.1. Multiphase CT and CTLP patient image series

Forty consecutive 4-phase CT examinations of the upper abdomen and 40 consecutive CTLP studies were retrospectively studied. All multiphase CT examinations included a non-enhanced CT (NECT) helical scan from the diaphragm to iliac crest, followed by contrast enhanced CT (CECT) helical scans at arterial, hepatic and delayed phase. CTLP acquisition protocol comprised 35 helical scans acquired in shuttle mode with temporal separation of 1.7 s. The length of imaged abdominal region in CTLP studies was 14 cm along z-axis and at least the 1st pass was acquired prior to contrast media arrival. All examinations had been performed on a General Electric Revolution HD CT scanner (GE Healthcare, Waukesha, WI, U.S.A). The acquisition protocols employed are shown in Table 1. The study was approved by the local institutional review board.

2.2. Measurement of tissue CT number increase in contrast enhanced CT scans

The CT number of primarily exposed radiosensitive organs/tissues i.e. liver, spleen, pancreas, kidneys, stomach, esophagus, intestine, red bone marrow, adrenals and muscle were recorded by positioning regions of interest (ROIs) on healthy tissue parenchyma in corresponding unenhanced and contrast-enhanced CT images. ROIs were appropriately set by two experienced CT radiologists avoiding large vessels and mean organ CT number values were recorded for each image set. ROIs on large organs with sufficient parenchyma (i.e. liver, spleen, and kidneys) were circular with an area of 2-3 cm^2. ROIs on pancreas, stomach, esophagus, intestine, red bone marrow, muscle and adrenals were freehand with area of 1-2 cm^2. For each patient, the CT number of an organ was determined for each different image dataset (i.e. acquired in different acquisition phase) using identical ROI in size and shape placed in exactly the same anatomical location. Corresponding CT number measurements obtained by the two radiologists differed by less than 6%. The increase of CT number (ΔCT) was derived for each organ and CECT phase. Namely, 3 values of ΔCT corresponding to the arterial, portal and delayed phase were obtained for each 4-phase patient CT study. Similarly, 34 ΔCT values were recorded for each patient CTLP study assuming the first pass was acquired prior to contrast medium arrival to tissues.

Table 1
Typical imaging protocols of liver multiphase CT and dynamic liver perfusion CT.

Acquisition parameters	Liver multiphase CT	Dynamic liver perfusion CT
Tube voltage (kV)	120	100
mA modulation (min mA/max mA)	yes (150/650)	no (150–200)[a]
Rotation time (s)	0.5	0.4
Beam collimation (mm)	40	40
pitch	0.984	1.375
Filter	Large body	Large body
Imaged volume length	22	14
Number of scans	3–4	35
Pass duration (s)	n/a	1.7
Total examination time (sec)	n/a	59
Reconstructed slice width (mm)	1.25/3.75	1.25/5
Adaptive Statistical Iterative Reconstruction (%)	50	50
Iodine administered (ml)	1 ml/kg of body weight	20 ml + 0.8 ml/kg of body weight
Iodine concentration (mg I/ml)	370	370
Iodine injection rate (ml/sec)	3	5

[a] Constant mA set at 150, 175 and 200 mA for normal, overweight and obese patients, respectively.

2.3. Estimation of tissue iodine uptake during scan acquisition

The iodine uptake in primarily exposed tissues in % w/w, at the time of each CT scan acquisition, was estimated from the recorded increase of CT number and previously published plots of CT number enhancement against iodine concentration of aqueous solutions [13].

2.4. Determination of organ doses and effective dose from NECT scans involved in MPCT and CTLP studies

The Monte Carlo N-particle transport code (MCNP, version 4C2) was employed to simulate CT exposures performed on the General Electric Revolution HD CT scanner (GE Healthcare, Waukesha, WI, U.S.A) installed at our institution. The x-ray spectra produced at 100 kV and 120 kV were obtained from Boone and Seibert [14]. The exposure geometry and the size/shape/material of beam filters employed during liver CT exposures were appropriately represented. The exposure parameters of the standard acquisition protocols presented in Table 1 were considered. The scanning length of each simulated CT exposure was defined taking into account the over-scanning effect [15].

The BodyBuilder software package (White Rock Science, White Rock, NM, USA) was used to develop an androgynous mathematical anthropomorphic phantom that mimics the size and internal anatomy of the average adult individual. All radiosensitive organs are represented in the generated phantom. The average adult was assumed with a body-mass index (BMI) of 23 kg/cm^2 with anteroposterior (AP) and lateral (L) abdominal dimensions of 20 and 40 cm, respectively. The effective abdominal diameter of the 'average adult' phantom was calculated as the square root of the product of AP and L dimensions to be 28.3 cm. To simulate individuals of increased size, two additional mathematical anthropomorphic phantoms were produced with BMI values of 25 and 28 kg/m^2 by adding 1- and 2-cm thick layers of fat tissue around the trunk of the 'average adult' phantom. The effective abdominal diameters of these phantoms were calculated to be 30.4 and

Table 2
Organ doses from NECT scans during MPCT and CTLP studies [data normalized to free-in-air CTDI (mGy/100mAs measured at isocenter).

Organ/tissue	NECT exposure during MPCT (120 kV, pitch = 0.984, imaged volume = 22 cm)			NECT exposure during CTLP (100 kV, pitch = 1.375, imaged volume = 14 cm)		
	Average adult (ED[a] = 28.3 cm)	Overweight Adult (ED = 30.4 cm)	Obese adult (ED = 32.5 cm)	Average adult (ED = 28.3 cm)	Overweight Adult (ED = 30.4 cm)	Obese adult (ED = 32.5 cm)
Bladder	0.034	0.031	0.028	0.012	0.011	0.010
Brain	0.000	0.000	0.000	0.000	0.000	0.000
Breast	0.098	0.065	0.035	0.038	0.025	0.013
Colon	0.215	0.191	0.169	0.059	0.055	0.049
Esophagus	0.206	0.185	0.161	0.086	0.075	0.065
Gonads	0.037	0.034	0.030	0.012	0.009	0.006
Liver	0.540	0.479	0.425	0.305	0.269	0.234
Lung	0.059	0.054	0.049	0.016	0.015	0.014
Red bone marrow	0.102	0.095	0.086	0.058	0.047	0.037
Salivary glands	0.025	0.019	0.017	0.004	0.004	0.004
Skeleton	0.304	0.281	0.257	0.138	0.126	0.115
Skin	0.114	0.117	0.118	0.051	0.053	0.053
Stomach	0.563	0.504	0.447	0.328	0.288	0.252
Thyroid	0.020	0.017	0.015	0.007	0.006	0.005
Remainder tissues						
Adrenal	0.529	0.471	0.413	0.303	0.262	0.226
Gall bladder	0.508	0.467	0.427	0.298	0.269	0.240
Heart	0.232	0.208	0.186	0.059	0.054	0.050
Kidney	0.612	0.548	0.483	0.369	0.324	0.282
Lymphatic nodes	0.001	0.001	0.001	0.001	0.001	0.001
Muscle	0.152	0.147	0.215	0.034	0.066	0.096
Oral mucosa	0.014	0.012	0.009	0.005	0.005	0.005
Pancreas	0.490	0.430	0.377	0.279	0.242	0.207
Prostate	0.022	0.018	0.016	0.007	0.006	0.005
Small Intestine	0.233	0.209	0.186	0.065	0.060	0.054
Spleen	0.525	0.471	0.422	0.308	0.271	0.239
Thymus	0.206	0.185	0.161	0.086	0.075	0.065
Uterus	0.060	0.056	0.052	0.019	0.018	0.016

[a] ED = effective diameter.

Table 3
Regression equations of absorbed dose increase (%) against iodine uptake (%) for primarily exposed organs (%DI = a · %IU).

Organ	CT scan at 100 kV		CT scan at 120 kV	
	a coefficient	R^2	a coefficient	R^2
Liver	69.3	0.995	72.4	0.974
Stomach	102.7	0.999	107.1	0.999
Intestine	77.0	0.997	78.2	0.993
Esophagus	100.8	0.995	97.5	0.974
Red bone marrow	83.7	0.999	96.0	0.999
Kidneys	101.8	0.999	102.5	0.999
Spleen	85.6	0.996	95.4	0.994
Adrenals	105.4	0.998	107.9	0.995
Pancreas	82.0	0.997	92.3	0.988
Muscle	112.2	0.999	110.6	0.998

32.5 cm, respectively.

The BodyBuilder software categorizes organs/tissues as either 'adult soft tissue', 'skeleton', or 'lung' with standard elemental composition and density to imitate the corresponding human tissues. Assuming the standard preset elemental composition and density of each organ/tissue, organ doses normalized to computed tomography dose index measured free-in-air ($CTDI_{free\text{-}in\text{-}air}$) at isocenter were determined for a) the NECT exposure of the multi-phase liver CT examination and b) the 1st pass of a CTLP study (i.e. prior to contrast arrival).

2.5. The effect of iodine concentration on absorbed dose to iodinated organs from CT exposure

Monte Carlo simulations of CT exposures on the mathematical anthropomorphic phantom representing the average adult were repeated assuming iodine concentration within each organ/tissue to be 0.1, 0.2, 0.3 and 0.4% w/w. The elemental composition of organs was appropriately modified for each of these simulation experiments. The absorbed dose to each organ for different iodine uptake was derived for exposures at 100 and 120 kV. Plots of % absorbed dose increase (%DI) against % iodine uptake (%IU) were produced and corresponding regression equations were determined for each imaged organ and X-ray beam employed.

2.6. Determination of cumulative organ doses and effective dose from MPCT and CTLP studies

Organ dose data for each CECT scan were calculated from the dose derived for the corresponding NECT scan by considering the dose increase to each organ due to the iodine tissue uptake (% w/w) at the time of scan acquisition. Cumulative organ dose data for the standard 3-phase and 4-phase abdominal CT study was derived by summing up the contribution of the first 3 and 4 scans, respectively. Similarly, cumulative organ dose data for the standard CTLP study was derived by summing up the contribution of each of the 35 scans comprising the study. The mean mAs value recorded in patients with effective abdominal diameter close to 28.3, 30.4 and 32.5 cm were considered to derive patient size-specific absolute values of organ doses from multiphase CT and CTLP studies. Effective dose values from 3- and 4-phase CT liver studies as well as CTLP study were estimated using the estimated organ doses and the formulation adopted by the International Commission on Radiological Protection [16].

3. Results

Normalized organ dose data for the NECT exposure involved in standard MPCT of upper abdomen and the NECT exposure involved in CTLP examination (i.e. 1st pass) are presented in Table 2 for different

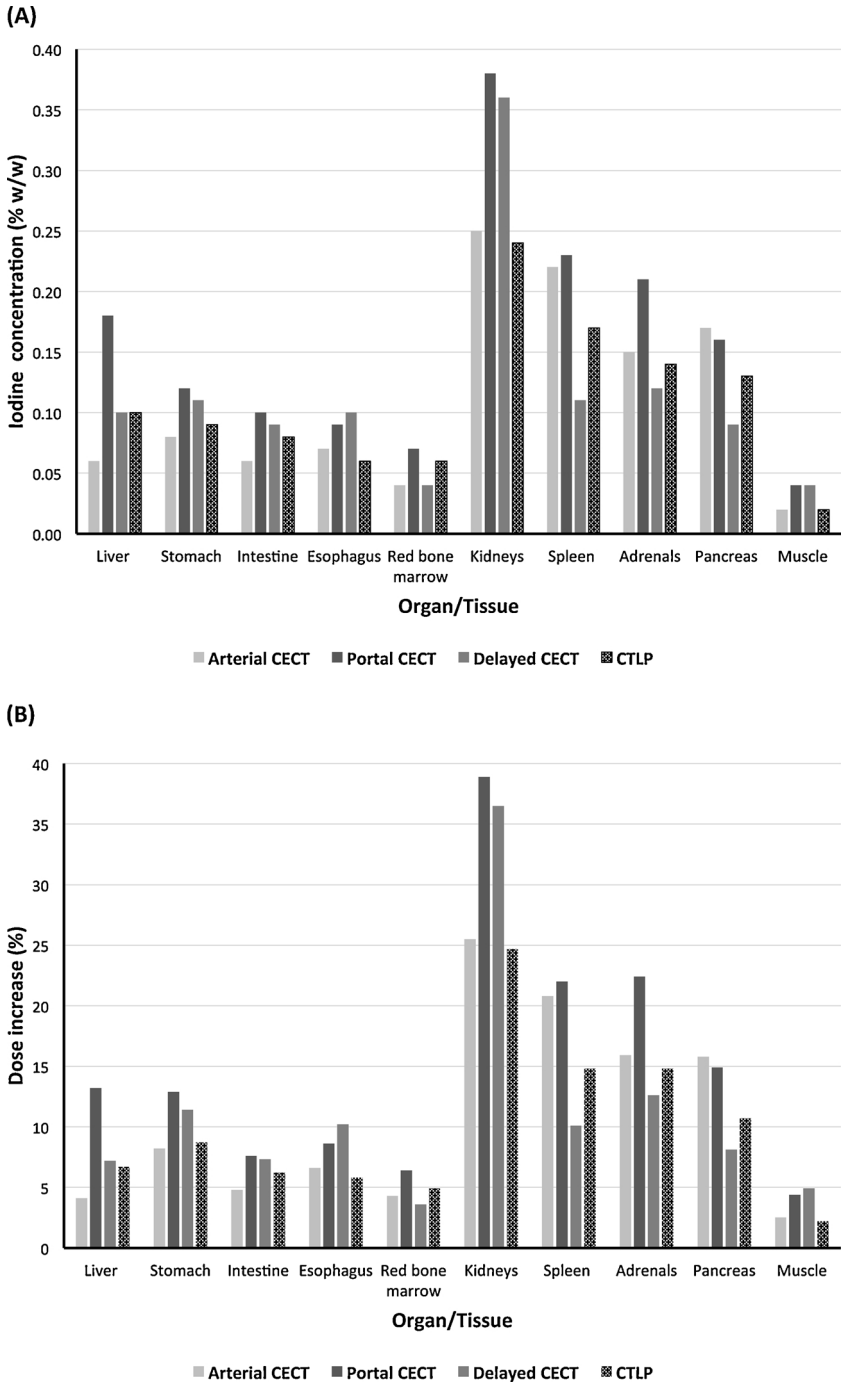

Fig. 1. Mean iodine concentrations (% w/w) of primarily exposed organs/tissues during acquisition of CECT scans involved in MPCT and during acquisition of CTLP studies (A) and corresponding organ dose % increases (B) due to the presence of iodinated contrast uptake.

body sizes. The tissues receiving the highest amount of radiation dose from either study were found to be kidney, stomach, liver, adrenals and spleen.

The regression equations of absorbed dose increase % against iodine uptake for each primarily exposed organ are presented in Table 3. The linear regression coefficient (% dose increase/% I uptake) was found to vary considerably between organs ranging from 69.3 to 112.

Mean iodine concentrations (% w/w) of primarily exposed organs/tissues during acquisition of CECT scans involved in MPCT and CTLP studies and corresponding organ dose % increase are presented in Fig. 1. The higher iodine uptake during CECT acquisitions and associated increase in absorbed dose was observed for kidneys, spleen, adrenals, pancreas, stomach and liver.

Absolute organ dose-based effective dose estimates for 3-phase and 4-phase CT of upper abdomen and for CTLP examination are presented in Table 4 for different patient-body sizes. Estimates have been derived taking into account the effect of iodine uptake on dose absorption. Corresponding effective dose estimates derived without taking into account the contrast-induced increase of organ doses are also presented for comparison. For an average size adult the radiation burden from CTLP was found to be 25% higher than the 3-phase and 7% lower than the 4-phase CT. For overweight patients, CTLP was found to be less dose burdening than either 3- and 4-phase CT.

Table 4
Comparison of cumulative effective dose from 3- and 4-phase CT of upper abdomen against CTLP.

	Effective dose (mSv)			% Difference	
Patient effective diameter (cm)/ BMI (kgr/m^2)	3-phase CT of upper abdomen	4-phase CT of upper abdomen	CTLP	(CTLP)-(3-phase CT)/ (3-phase CT)	(CTLP)-(4-phase CT)/ (4-phase CT)
28.2/23	20.6 (19.5)[a]	27.7 (26.1)[a]	25.8 (23.9)[a]	25%	−7%
30.3/25	27.0 (25.5)[a]	36.1 (34.0)[a]	26.3 (24.4)[a]	−3%	−27%
32.2/28	31.0 (29.4)[a]	41.5 (39.0)[a]	25.9 (24.0)[a]	−17%	−38%

[a] Estimates of effective dose if iodine uptake is not taken into account.

Table 5
Comparison of current results on effective dose from CTLP with corresponding previously published data.

Study (publication year)	CT scanner	kV	Phases	Coverage (cm)	Effective dose (mSv)
Zhang et al. [17]	Philips Brilliance iCT	80	60	8	28.5
Gawlitza et al. [4]	Siemens Somatom FORCE	70/80	18	22.4	22.6
Lee et al. [18]	Siemens Somatom Definition	100	36	10	26.3
Fischer et al. [19]	Siemens Somatom Definition Flash	80/100	30–36	14.8–18.2	32–45
Cros et al. [20]	Toshiba Aquilion One	100	23	16	25.7
Current study	GE Revolution HD	100	35	14	25.8

4. Discussion

Latest technical advancements in CT technology improved the quality of dynamic CT imaging procedures and triggered a debate regarding the potential of CTLP to be considered as an alternative of, or even replace, the standard MPCT of upper abdomen in the diagnosis/ follow up of liver lesions [1]. Apart from the assessment and comparison of the diagnostic utility of CTLP and MPCT regarding liver lesions which is more important and clinically relevant, the patient radiation burden associated with these two alternative diagnostic procedures should be also accurately determined, compared and taken into consideration [1,8]. Both above liver CT imaging procedures involve administration of iodinated contrast medium which has been recently reported to considerably affect radiation dose absorption by exposed tissues. To our knowledge, this is the first study comparing radiation burden from routine multi-phase CT and CTLP studies taking into account the increase of radiation dose to exposed tissues due to iodine uptake at the time of exposure.

Absorbed radiation doses to exposed radiosensitive organs/tissues from the typical NECT exposures involved in multi-phase CT of upper abdomen and CTLP were determined for three different patient body sizes using Monte Carlo simulation methods. Organ dose data were also derived for identical exposures following iodinated contrast medium administration (i.e. CECT exposures involved in multi-phase CT and CTLP procedures) taking into account the iodine uptake of tissues at the time of acquisition of involved scans and its effect on dose. Organ dose-based estimates of effective dose from 3-phase CT, 4-phase CT and CTLP studies were derived by summing up the contribution of NECT and CECT scans involved in each of these procedures. Provided dosimetric data allow patient-size specific comparison of radiation burden associated with multi-phase CT and CTLP studies. As shown in Table 4, the effective dose from CTLP was found lower than 4-phase CT irrespective of patient body size. Compared to 3-phase CT, the radiation burden from CTLP was found to be higher for average size patients but again lower for overweight patients. Our results demonstrate that CTLP may be more dose efficient than 4-phase CT and occasionally even than 3-phase CT when a modern CT scanner is employed. This is in accordance to recently published data by Gawlitza et al [4]. Despite a different vendor CT scanner and different acquisition protocols were considered in that study, similar radiation burden from the standard 3-phase liver CT and low kV CTLP studies was reported. However, the iodine uptake effect on dose was not encountered in that study while the applicability of the low kV CTLP acquisition protocol on overweight patients was not investigated. Previously published data on effective dose from CTLP performed on modern CT scanners are presented for comparison with current findings in Table 5. It is noted that the number of scans acquired, the coverage and exposure settings strongly influence the cumulative radiation burden to a patient subjected to CTLP. The effective dose to an average size patient subjected to CTLP as determined in the present study falls in the lower range of previously reported values.

The underestimation of organ doses from a CECT exposure, if iodine uptake is not encountered, was found to vary between organs and imaging phase, as shown in Fig. 1. This is to be expected due to the dependence of iodine uptake on a) the ability of each tissue to uptake the administered iodinated contrast and b) the time of scan acquisition along the contrast administration timeline. The mean underestimation of organ doses from a CECT exposure, if iodine uptake is not encountered, was found to range 2.2%–38.9% depending on the tissue ability to uptake iodine and the time of acquisition. It is noted that latter values are average values over the studied patient cohort and the maximum underestimation for a specific organ in a patient may approach 70%. The underestimation in effective dose from a CECT exposure was found to range 0–15% depending on acquisition timing, while the resulted underestimation of cumulative effective dose from 3-phase CT, 4-phase CT and CTLP involving several NECT and CECT studies was found to be 5%, 6% and 7%, respectively.

In the current study, multi-phase CT and CTLP were dosimetrically compared in terms of organ dose-based effective dose estimates. The concept of effective dose was introduced as a risk-related radiological protection quantity, averaged over gender and age, to be used for radiation protection of occupationally exposed personnel [16]. Therefore its application for quantification of the radiation-related stochastic

health risk of a patient cohort subjected to a medical exposure has been strongly challenged [10,11,21]. Nevertheless, most investigators agree on its utility for comparing radiation detriment from different radiodiagnostic examinations [10,11].

The main limitation of the current study originates from the use of stylized mathematical anthropomorphic phantoms to determine organ dose data from CT scans involved in multi-phase CT and CTLP studies. There is a considerable variability in shape/size of body and organs between individuals that may introduce uncertainties in provided organ dose data. In the current study dosimetric data were derived for three different body sizes to minimize this source of uncertainty. Another source of uncertainty originates from the method employed to determine the absorbed dose to iodinated organs/tissues from CECT exposures. Organ doses were determined by estimating iodine uptake at the time of scan acquisition through the CT number increase with respect to NECT images assuming that all studied radiosensitive organs/tissues are water-equivalent prior to iodine uptake. However, different soft tissue types e.g. liver, kidney, spleen etc might slightly differ from water regarding the ability to absorb X-rays. Therefore, there is an uncertainty in the estimated doses to organs after iodinated contrast uptake which, however, is not expected to exceed 5%. Also, the iodine uptake of organs not included in imaged body volume could not be determined. Therefore, the increase of dose to these organs due to the iodine uptake could not be substantiated. However, not primarily exposed organs tissues receive much lower radiation dose and therefore the introduced uncertainty in effective dose estimates is expected to be minor.

5. Conclusions

Modern CT technology may allow acquisition of CTLP studies at comparable or even lower patient radiation burden compared to routine multi-phase liver CT imaging. Current results may alleviate radiation-related concerns regarding the use of CTLP for the detection/follow up of liver lesions as an alternative of the routine multiphase CT of upper abdomen.

Acknowledgements

Authors would like to thank GE Healthcare (Waukesha, WI, U.S.A) for providing the required technical information regarding the shape/size/material of beam filters selectable on the General Electric Revolution HD CT scanner.

References

[1] S.H. Kim, A. Kamaya, J.K. Willmann, CT perfusion of the liver: principles and applications in oncology, Radiology 272 (2014) 322–344.
[2] S. Kaufmann, T. Horger, A. Oelker, et al., Characterization of hepatocellular carcinoma (HCC) lesions using a novel CT-based volume perfusion (VPCT) technique, Eur. J. Radiol. 84 (2015) 1029–1035.
[3] S. Gordic, G.D. Puippe, B. Krauss, et al., Correlation between dual-energy and perfusion CT in patients with hepatocellular carcinoma, Radiology 280 (2016) 78–87.
[4] J. Gawlitza, H. Haubenreisser, M. Meyer, et al., Comparison of organ-specific-radiation dose levels between 70 kVp perfusion CT and standard tri-phasic liver CT in patients with hepatocellular carcinoma using a Monte-Carlo-simulation-based analysis platform, Eur. J. Radiol. Open 3 (2016) 95–99.
[5] G. Brix, U. Lechel, E. Nekolla, et al., Radiation protection issues in dynamic contrast-enhanced (perfusion) computed tomography, Eur. J. Radiol. 84 (2015) 2347–2358.
[6] R. Goetti, C.S. Reiner, A. Knuth, et al., Quantitative perfusion analysis of malignant liver tumors: dynamic computed tomography and contrast-enhanced ultrasound, Invest. Radiol. 47 (2012) 18–24.
[7] O.M. Topcuoğlu, M. Karçaaltıncaba, D. Akata, et al., Reproducibility and variability of very low dose hepatic perfusion CT in metastatic liver disease, Diagn. Interv. Radiol. 22 (2016) 495–500.
[8] X. Wang, T. Henzler, J. Gawlitza, Image quality of mean temporal arterial and mean temporal portal venous phase images calculated from low dose dynamic volume perfusion CT datasets in patients with hepatocellular carcinoma and pancreatic cancer, Eur. J. Radiol. 85 (2016) 2104–2110.
[9] F. Morsbach, B.R. Sah, L. Spring, et al., Perfusion CT best predicts outcome after radioembolization of liver metastases: a comparison of radionuclide and CT imaging techniques, Eur. Radiol. 24 (2014) 1455–1465.
[10] International Commission on Radiological Protection Managing patient dose in multi-detector computed tomography (MDCT), ICRP publication 102, Ann. ICRP 37 (1) (2007).
[11] American Association of Physicists in Medicine (AAPM). The measurement, reporting and management of radiation dose in CT. Report of AAPM Task Group 23 (2008).
[12] W.A. Kalender, Dose in x-ray computed tomography, Phys. Med. Biol. 59 (2014) R129–R150.
[13] K. Perisinakis, A. Tzedakis, K. Spanakis, et al., The effect of iodine uptake on radiation dose absorbed by patient tissues in contrast enhanced CT imaging: implications for CT dosimetry, Eur. Radiol. 28 (2018) 151–158.
[14] J.M. Boone, J.A. Seibert, An accurate method for computer-generating tungsten anode x-ray spectra from 30 to 140 kV, Med. Phys. 24 (1997) 1661–1670.
[15] A. Tzedakis, J. Damilakis, K. Perisinakis, et al., The effect of z overscanning on patient effective dose from multidetector helical computed tomography examinations, Med. Phys. 32 (2005) 1621–1629.
[16] International Commission of Radiological Protection (ICRP), The 2007 recommendations of the international commission on radiological protection. ICRP publication 103, Ann. ICRP 37 (2–4) (2007).
[17] C.Y. Zhang, Y.F. Cui, C. Guo, et al., Low contrast medium and radiation dose for hepatic computed tomography perfusion of rabbit VX2 tumor, World J. Gastroenterol. 21 (2015) 5259–5270.
[18] D.H. Lee, J.M. Lee, E. Klotz, et al., Multiphasic dynamic computed tomography evaluation of liver tissue perfusion characteristics using the dual maximum slope model in patients with cirrhosis and hepatocellular carcinoma: a feasibility study, Invest. Radiol. 51 (2016) 430–434.
[19] M.A. Fischer, N. Kartalis, A. Grigoriadis, et al., Perfusion computed tomography for detection of hepatocellular carcinoma in patients with liver cirrhosis, Eur. Radiol. 25 (2015) 3123–3132.
[20] M. Cros, J. Geleijns, R.M. Joemai, et al., Perfusion CT of the brain and liver and of lung tumors: use of Monte Carlo simulation for patient dose estimation for examinations with a cone-beam 320-MDCT Scanner, AJR Am. J. Roentgenol. 206 (2016) 129–135.
[21] D.J. Brenner, Effective dose: a flawed concept that could and should be replaced, Br. J. Radiol. 81 (2008) 521–523.